

Dynamic Rate and Power Adaptation for Provisioning Class-Based QoS in Cellular Multirate WCDMA Systems

Dong In Kim, *Senior Member, IEEE*, Ekram Hossain, *Member, IEEE*, and Vijay K. Bhargava, *Fellow, IEEE*

Abstract—This paper addresses the problem of dynamic link adaptation under multiple quality-of-service (QoS) constraints in cellular wideband code-division multiple-access (WCDMA) systems. A novel dynamic joint rate and power adaptation framework is proposed for downlink data transmission in a multicell variable spreading factor (VSF) WCDMA system where the different classes of users have different signal-to-interference ratio (SIR) requirements. Based on a general downlink SIR model, the problem of optimal dynamic rate and power adaptation under multiple SIR constraints is also formulated, for which the rate and power allocation can be found by an exhaustive search. Two schemes, namely, *near-optimal* and *suboptimal* schemes, are proposed for implementation-friendly dynamic rate and power adaptation. Performance of dynamic joint rate and power adaptation under the proposed framework is evaluated under random micro-mobility model with uncorrelated long-term fading and a directional micro-mobility model with correlated long-term fading in a cellular WCDMA environment.

Index Terms—Dynamic rate and power adaptation, multicell multirate wideband code-division multiple-access (WCDMA) systems, class-based quality of service (QoS), priority-based rate adaptation.

I. INTRODUCTION

WIDEBAND code-division multiple-access (WCDMA)-based air interface is being designed to provide high speed packet data services with differentiated quality-of-service (QoS) support in the future-generation wireless networks (e.g., 3G enhancements and 4G wireless networks) [1]. In a WCDMA system, the transmission rate and the power corresponding to the different mobile users can be dynamically varied depending on the variations of the channel condition to improve the spectral efficiency while meeting the QoS requirements for the diverse

multimedia applications. This form of dynamic link adaptation would be the key to implementing a class-based QoS framework that enables sharing of radio resources among users with different QoS requirements in a fair and efficient manner [2].

The data transmission rate in the forward link physical layer of a WCDMA system can be controlled by using the variable spreading factor method or the multicode method [3]. This paper proposes a novel dynamic joint rate and power adaptation framework for downlink data transmission in multicell variable spreading factor (VSF) WCDMA systems where the mobile data users are assumed to have *different* signal-to-interference ratio (SIR) (and, hence, different bit-error rate) requirements. Channel impairments due to multiuser interference as well as time-varying and location-dependent channel characteristics are incorporated in the proposed framework through a general SIR model. Using this SIR model, the problem of *optimal* dynamic rate and power adaptation under multiple SIR constraints in a multicell WCDMA system is formulated as an exhaustive search over the solution space of a system of linear equations. The optimality criterion is the maximization of the *average number of radio link level frames transmitted per frame-time*¹ under multiple SIR constraints and constrained power budget in the base station transmitter.

The exhaustive search-based optimal dynamic rate and power adaptation would be prohibitively complex to implement due to exponential time-complexity. A simpler rate and power adaptation scheme with comparable performance characteristics can be devised using a heuristic-based power allocation² along with a link quality-based rate allocation strategy. Two such schemes, namely, *near-optimal* and *suboptimal* schemes are proposed for dynamic rate and power adaptation on a *joint-cell* basis and *single-cell* basis, respectively.

Specifically, the proposed *suboptimal* rate and power allocation scheme may make the dynamic rate and power allocation on a frame-by-frame basis feasible and manageable in a cellular WCDMA network without much control overhead. However, link quality-based rate adaptation under constrained SIR may result in an uneven rate allocation among the users in the different service classes, and consequently, users with higher SIR requirements (presumably with more stringent delay requirements) may experience lower throughput performance compared to those with relatively lower SIR requirements.

¹In this paper, this is referred to as the sum-rate throughput.

²This power allocation refers to the allocation of power among the base station transmitters in the different cells for data transmission in the downlink to the mobiles.

Manuscript received March 13, 2002; revised April 30, 2003; accepted May 26, 2003. The editor coordinating the review of this paper and approving it for publication is B. Li. This work was supported in part by Simon Fraser University under the PRG Research Grant and in part by the Natural Sciences and Engineering Research Council (NSERC) of Canada. This work was presented in part at the 2003 IEEE International Conference on Communications, Anchorage, AK, May 2003.

D. I. Kim is with the School of Engineering Science, Simon Fraser University, Burnaby, BC V5A 1S6, Canada (e-mail: dikim@sfu.ca).

E. Hossain is with the Department of Electrical and Computer Engineering, University of Manitoba, Winnipeg, MB R3T 5V6, Canada (e-mail: ekram@ee.umanitoba.ca).

V. K. Bhargava is with the Department of Electrical and Computer Engineering, University of British Columbia, Vancouver, BC V6T 1Z4, Canada.

Digital Object Identifier 10.1109/TWC.2004.833492

Therefore, the proposed scheme is enhanced to integrate priority-based rate adaptation with link quality-based dynamic rate adaptation to provide a more flexible dynamic link adaptation framework.

Performance of dynamic joint rate and power adaptation in the proposed framework is analyzed for both *random* and *directional* user micro-mobility models in a multicell WCDMA environment. The long-term channel fading is assumed to be uncorrelated and correlated, respectively, for the random and the directional micro-mobility models. Since the short-term fading (i.e., multipath fading) changes more rapidly compared to the long-term fading (i.e., path loss and shadowing), it is assumed to be independently varying.

The organization of the rest of the paper is as follows. Section II presents the background and motivation of the work. Based on a general SIR model for downlink data transmission in a multicell VSF WCDMA system, the problem of optimal rate and power allocation under multiple SIR constraints is formulated in Section III. Section IV presents the suboptimal joint rate and power allocation strategy for dynamically adjusting the transmission rate and the transmission power corresponding to the mobiles in the different QoS classes. In Section V, radio link level throughput (in terms of the average number of radio link level frames transmitted per frame-time) is investigated analytically for suboptimal joint rate and power adaptation under the proposed framework. The simulation model along with the simulation and the analytical results are presented in Section VI. Conclusions are stated in Section VII.

II. BACKGROUND AND MOTIVATION

The problem of optimal rate and power adaptation for *uplink* packet data transmission in a single-cell multirate CDMA system was addressed in [4] and the optimal centralized adaptive rate and power control strategy to maximize the total average weighted throughput was determined. With the objective of maximizing the throughput and with the constraints on maximum power and/or minimum rate, the problem of jointly controlling the user power and data rates for *uplink* data transmission in a *single-cell* CDMA system was formulated as a constrained optimization problem in [5]–[7]. In [8], the throughput maximization problem for CDMA *uplinks* was formulated as an optimization problem in terms of the spreading gains and the transmit powers of the users.

The problem of joint rate and power adaptation under single SIR constraint and constrained power budget for *downlink* data transmission in a multicell and multirate CDMA system was addressed in [9]. This paper extends the work in [9] by considering multiple SIR constraints in a class-based QoS framework. The work in [10] is particularly relevant to this work where a dynamic bandwidth scheduling scheme was proposed to implement a class-based QoS framework for a CDMA air interface. In such a framework, each service class offers some characteristic performance behavior (or group behavior) and mobile user applications can select a service class based on their QoS requirements and pricing schemes. Although the dynamic rate adjustment in the proposed bandwidth scheduling scheme was based on the elasticities of the service classes and the path loss factors

TABLE I
LIST OF KEY NOTATIONS

g_j ($j = 0, \dots, J$)	No. of mobiles in cell j
$m_i^{(j)}$	Transmission rate allocated to i th mobile in cell j
$P_{b,i}^{(j)}$	Power allocated to i th mobile in cell j corr. to the basic rate v_1
$m_i^{(j)} \times P_{b,i}^{(j)}$	Total power allocated to i th mobile in cell j
$\eta_{j'/j}(i)$	Inter-cell interference factor corr. to the transmission to i th mobile in cell j
P_c	Pilot signal transmission power
$P_{B,j}$	Total power budget available at the j th BS
P_B	Average power budget for BS transmitters per cell
$\beta_{j'/j}$	Ratio of $P_{B,j'}$ and $P_{B,j}$
$(SIR)_o$	Target SIR for mobiles with lowest SIR requirement (i.e., target SIR for service class 1)
$(SIR)_{o,q}$ ($q = 1, 2, \dots, Q$)	Target SIR for service class q
$\mu_i^{(j)}$	Effective interference factor for i th mobile in cell j

corresponding to the mobiles, the specific SIR requirements for each class of users were not explicitly taken into account.

More comprehensive and general channel model and user micro-mobility models are adopted in the joint dynamic rate and power adaptation framework proposed in this paper. As a result, the impacts of the radio channel parameters and the user micro-mobility patterns on the radio link level performance under dynamic rate adaptation can be investigated. Also, the concepts of radio link quality-based dynamic rate adaptation and user priority (or requirements)-based dynamic rate adaptation are integrated into a single framework. To this end, an analytical approach is presented for approximate evaluation of radio link level performance under dynamic rate adaptation with multiple SIR constraints. The proposed dynamic rate and power allocation framework would enable us to evaluate the higher layer protocol (e.g., transmission control protocol (TCP) [11]) performance under dynamic radio link adaptation with QoS differentiation and better understand the interlayer protocol interactions in multirate cellular WCDMA networks.

III. MODELING OF DOWNLINK SIR AND OPTIMAL RATE AND POWER ALLOCATION

Table I lists the notations for the key parameters to be used in the downlink SIR modeling.

A. Modeling of Downlink SIR

A variable rate downlink packet access for VSF WCDMA (with the basic spreading gain given by N chips per bit) is considered where the transmission rates can be selected from the set $\{r_0, r_1, \dots, r_\varphi\}$. With $r_m = mr_1$ ($m = 0, 1, \dots, \varphi$), in the case of rate r_m , the spreading gain is reduced to N/m chips per bit.

With the radio propagation modeled by intercell interference, path loss, shadowing and multipath fading and assuming a uniform spatial distribution of the mobiles in the cells, the downlink SIR for the i th mobile in cell j ($j = 0, 1, \dots, J$) can be formulated as follows [9]:

$$(\text{SIR})_{o,i}^{(j)} = \frac{P_{b,i}^{(j)} N}{P_{B,j} [(1 - \nu) + \sum_{j' \neq j} \beta_{j'/j} \cdot \eta_{j'/j}(i)]}. \quad (1)$$

In (1), $P_{B,j}$ is the total transmission power at the j th base station (BS) $_j$ and is given by

$$P_{B,j} = \sum_{i=1}^{g_j} m_i^{(j)} P_{b,i}^{(j)} + P_c \quad (2)$$

where g_j is the number of mobiles in cell j ($j = 0, 1, \dots, J$), $m_i^{(j)} \in \{0, 1, \dots, \varphi\}$ denotes the rate allocation to the k th mobile in cell j , and $P_{b,i}^{(j)}$ is the power allocation at basic rate (so that the total power allocation to the i th mobile in cell j is $m_i^{(j)} P_{b,i}^{(j)}$), $\beta_{j'/j} = P_{B,j'}/P_{B,j}$, and P_c is the pilot signal transmission power.

In (1), ν represents the downlink in-cell orthogonality factor ($\nu = 1$ implies perfectly orthogonal in-cell mobiles) to account for the interpath interference due to multipath³ and $\eta_{j'/j}(i)$ is the intercell interference factor defined by

$$\eta_{j'/j}(i) \triangleq \frac{\zeta_i^{(j')} L_{j'}(j, i)}{\zeta_i^{(j)} L_j(j, i)}. \quad (3)$$

Here, $\zeta_i^{(j')}$ and $L_{j'}(j, i)$ denote the short-term and the long-term fading, respectively, in the link between (BS) $_{j'}$ and the i th mobile in cell j (tagged cell). $L_{j'}(j, i)$, as given by (4) below, models the log-normal shadowing and the distance-dependent attenuation (as the δ th power of the distance).

$$L_{j'}(j, i) = r_{i,j'}^{-\delta} \cdot 10^{\xi_{i,j'}/10}. \quad (4)$$

Defining the effective interference factor $\mu_i^{(j)}$ as

$$\mu_i^{(j)} = \left[(1 - \nu) + \sum_{j' \neq j} \beta_{j'/j} \cdot \eta_{j'/j}(i) \right], \quad (5)$$

the downlink SIR in (1) can be written as

$$(\text{SIR})_{o,i}^{(j)} = \frac{P_{b,i}^{(j)} N}{\mu_i^{(j)} P_{B,j}}. \quad (6)$$

Therefore, for given power allocations $\{P_{B,j} | j = 0, 1, \dots, J\}$ and $P_{b,i}^{(j)}$ (which are presumably fixed during each adaptation interval), the effective interference factor $\mu_i^{(j)}$ can be estimated by measuring $(\text{SIR})_{o,i}^{(j)}$ at the corresponding mobile. Based on the measured/estimated $\{\mu_i^{(j)}\}$, the SIR can be controlled to meet the different QoS requirements.

For optimal dynamic link adaptation the rate and power allocations need to be determined based on (1) and (2) so that the different SIR constraints are satisfied.

³In fact, ν depends on the location of the mobile and the characteristics of the multipath fading channel. For simplicity, the effect of mobile location on ν is not taken into account and a constant value of $\nu (< 1)$ is assumed here.

B. Optimal Rate and Power Adaptation

We assume that the multilevel QoS is defined over Q service classes with the target SIR for class q ($q = 1, 2, \dots, Q$) being $(\text{SIR})_{o,q}$. Then, for the optimal rate and power allocation the total number of transmitted frames $\sum_{j=0}^J \sum_{i=1}^{g_j} m_i^{(j)}$ during an adaptation interval⁴ is maximized subject to the following constraints on SIR and base station transmission power budget

$$(\text{SIR})_{o,i}^{(j)} \geq (\text{SIR})_{o,q} \quad \text{for } i \in I_q^{(j)}, \quad q = 1, 2, \dots, Q \quad (7)$$

$$\frac{1}{(J+1)} \sum_{j=0}^J P_{B,j} \leq P_B \quad (8)$$

where the index set $I_q^{(j)}$ is defined for all the mobiles in cell j with target $(\text{SIR})_{o,q}$, i.e., $\cup_{q=1}^Q I_q^{(j)} = \{1, 2, \dots, g_j\}$, and P_B is the average power constraint per cell (i.e., average power budget available at the base station transmitter for downlink data transmission).

If it is assumed that the target SIR for class q (i.e., $(\text{SIR})_{o,q}$) is related to the minimum target SIR (denoted by $(\text{SIR})_o$) by

$$\kappa_q \triangleq \log_2 \left[\frac{(\text{SIR})_{o,q}}{(\text{SIR})_o} \right], \quad q = 1, 2, \dots, Q, \quad \kappa_q \geq 0 \quad (9)$$

then *Proposition 1* serves as the basis to determine the optimal rate and power allocations under multiple QoS constraints (in terms of target SIRs).

Proposition 1: Given the set of rate allocations $\{m_i^{(j)}\}$, the global power allocations $\{P_{B,j}\}$ can be determined by solving the $(J+1)$ simultaneous linear equations in (10), where $\beta_j = P_{B,j}/P_c$ and $(\text{SIR})_{o,i}^{(j)} = 2^{\kappa_q} (\text{SIR})_{o,d}$ for $i \in I_q^{(j)}$, subject to the constraints $(\text{SIR})_{o,d} \geq (\text{SIR})_o$ and $1/(J+1) \sum_{j=0}^J \beta_j \leq P_B/P_c$. Note that, $(\text{SIR})_{o,d}$ here represents the minimum target SIR plus some margin, i.e., $(\text{SIR})_{o,d} = (\text{SIR})_o + \epsilon$ for a small value $\epsilon > 0$

$$\beta_j \left[N - (1 - \nu) \sum_{q=1}^Q 2^{\kappa_q} \left(\sum_{i \in I_q^{(j)}} m_i^{(j)} \right) (\text{SIR})_{o,d} \right] - \sum_{j' \neq j} \beta_{j'} \sum_{q=1}^Q 2^{\kappa_q} \left(\sum_{i \in I_q^{(j')}} m_i^{(j')} \eta_{j'/j}(i) \right) (\text{SIR})_{o,d} = N \quad j = 0, 1, \dots, J. \quad (10)$$

Proof of Proposition 1: Combining (5) and (6) with $\beta_{j'/j} = P_{B,j'}/P_{B,j}$, we obtain

$$N P_{b,i}^{(j)} = \left[(1 - \nu) P_{B,j} + \sum_{j' \neq j} P_{B,j'} \cdot \eta_{j'/j}(i) \right] (\text{SIR})_{o,i}^{(j)}. \quad (11)$$

Here, we assume a steady-state system condition where all the mobiles belonging to the same service class q , i.e., $\forall i \in I_q^{(j)}$ achieve the same downlink quality in terms of $(\text{SIR})_{o,i}^{(j)} = 2^{\kappa_q} (\text{SIR})_{o,d}$ [due to power allocation $P_{b,i}^{(j)}$ in

⁴The adaptation interval is assumed to be one frame-time in this paper.

proportion to the interference factor $\mu_i^{(j)}$ as in (6)]. This assumption holds for the optimal rate and power allocation where the downlink quality should be kept to the minimum required $(\text{SIR})_{o,q}$ for $\forall i \in I_q^{(j)}$.

Multiplying (11) by $m_i^{(j)}$ and summing up for $i = 1, 2, \dots, g_j$ and using (2) yields

$$N(P_{B,j} - P_c) = \left[(1 - \nu)P_{B,j} \sum_{i=1}^{g_j} m_i^{(j)} (\text{SIR})_{o,i}^{(j)} + \sum_{j' \neq j} P_{B,j'} \sum_{i=1}^{g_j} m_i^{(j)} \eta_{j'/j}(i) (\text{SIR})_{o,i}^{(j)} \right]. \quad (12)$$

Now, classifying all the mobiles in cell j into the subsets of each service class $\{I_q^{(j)} \mid q = 1, 2, \dots, Q\}$, where $\cup_{q=1}^Q I_q^{(j)} = \{1, 2, \dots, g_j\}$, and then substituting $(\text{SIR})_{o,i}^{(j)} = 2^{\kappa_q} (\text{SIR})_{o,d}$ into (12) for $\forall i \in I_q^{(j)}, q = 1, 2, \dots, Q$, (10) is obtained. ■

Based on the global power allocations $\{P_{B,j}\}$, the power allocations at basic rate $\{P_{b,i}^{(j)}\}$ can be determined from

$$P_{b,i}^{(j)} = \frac{1}{N} \left(2^{\kappa_q} \mu_i^{(j)} \right) P_{B,j} \cdot (\text{SIR})_{o,d} \quad (13)$$

for $i \in I_q^{(j)}$, when the effective interference factors $\{\mu_i^{(j)}\}$ are obtained using (5) with $\beta_{j'/j} = P_{B,j'}/P_{B,j}$. Here, it is assumed that the in-cell orthogonality factor ν and the intercell interference factors $\{\eta_{j'/j}(i)\}$ can be measured at the mobile units. Note that, the earlier formulation of the optimal rate and power allocation problem [in terms of (10) and (13)] is based on the channel conditions (e.g., $\nu, \{\eta_{j'/j}(i)\}$), SIR requirements (via $\{(\text{SIR})_{o,q} \mid q = 1, 2, \dots, Q\}$) and user classes and traffic loads (e.g., $\{n_q^{(j)}\}, \{g_j\}$).

Now, the power allocations $\{P_{B,j}\}$ and $\{P_{b,j}\}$ derived from (10) and (13) should be globally optimized by searching the rate combination $\{m_i^{(j)}\}$ across the $(J+1)$ cells that maximizes the sum of the transmission rates during a frame-time (or sum-rate throughput $\sum_{j=0}^J \sum_{i=1}^{g_j} m_i^{(j)}$). Since finding the optimal solution requires cycling through all possible assignments it would involve exponential time complexity [of $O(\varphi^{(g_0 + \dots + g_J)})$].

C. Near-Optimal Rate Adaptation

The complexity of exhaustive rate search can be reduced while presumably achieving close to the maximum sum-rate throughput by some “greedy” method for rate allocation in which maximum possible transmission rates are allocated to the mobiles experiencing better channel conditions. The channel condition for each mobile is characterized by the corresponding *effective interference factor* (i.e., $\mu_i^{(j)}$). Since $\mu_i^{(j)}$ s for the mobiles in the different cells depend on the power allocations at the base station transmitters, a heuristic-based power allocation is to be assumed so that these can be estimated using (5).

For this, let us define $n_q^{(j)} = |I_q^{(j)}|, q = 1, 2, \dots, Q$, where $g_j = \sum_{q=1}^Q n_q^{(j)}$ for $j = 0, 1, \dots, J$. Since the total transmission power at a base station could generally be allocated based on the number of users in each service class and the different

SIR requirements, the heuristic power allocations $\{P_{B,j}^*\}$ can be determined according to the following (see the Appendix):

$$P_{B,j}^* = \frac{\sum_{q=1}^Q 2^{\kappa_q} n_q^{(j)}}{\sum_{j'=0}^J \sum_{q=1}^Q 2^{\kappa_q} n_q^{(j')}} (J+1) P_B, \quad j = 0, 1, \dots, J \quad (14)$$

where * denotes explicitly the heuristic-based power allocation $P_{B,j}^*$ to distinguish it from the optimal power allocation $P_{B,j}$. This power allocation is based only on the number of users in the different cells and the corresponding SIR requirements. Then, using these power allocations, the effective interference factors $\{\mu_i^{(j)}\}$ can be estimated using (5).

Note that, if $\kappa_q = 0 \forall q$ (i.e., $(\text{SIR})_{o,q} = (\text{SIR})_o, q = 1, 2, \dots, Q$), the power allocations $\{P_{B,j}^*\}$ reduce to $P_{B,j}^* = (g_j)/(\sum_{j'=0}^J g_{j'}) (J+1) P_B, j = 0, 1, \dots, J$, as was in the case of common SIR requirement in [9].

The complexity of the rate search is reduced by allocating maximum allowable transmission rates to the mobiles in an ascending order of $(2^{\kappa_q} \mu_i^{(j)})$ for which feasible total power allocations are obtained by solving the $(J+1)$ linear equations in (10) and the sum-rate throughput is maximized. We refer to this as the near-optimal dynamic rate and power allocation. Note that the per-cell power allocations $\{P_{B,j}^*\}$ [as calculated using (14)] based on SIR requirements (i.e., $\{(\text{SIR})_{o,q} \mid q = 1, 2, \dots, Q\}$), user classes and traffic loads (e.g., $\{n_q^{(j)}\}, \{g_j\}$) are used only to determine the effective interference factors $\{\mu_i^{(j)}\}$ while the actual power allocations are obtained by solving the linear equations in (10). Since solving a set of $(J+1)$ linear equations has time complexity of $O(J+1)^3$, the rate and power allocation for this case has time complexity of $O(\varphi \cdot \sum_{j=0}^J g_j \cdot (J+1)^3)$.

The optimal and the near-optimal rate and power allocation require that the in-cell orthogonality factor ν and the intercell interference factors $\{\eta_{j'/j}(i)\}$ be *a priori* measured and estimated for each mobile in a cluster of cells. However, it would cause much control overhead, and therefore, a suboptimal method is proposed which performs dynamic rate and power allocation on a per-cell basis (rather than on a joint-cell basis) and, hence, makes fast dynamic link adaptation feasible from implementation point of view.

IV. SUBOPTIMAL RATE AND POWER ALLOCATION

A. Dynamic Link Adaptation Based on Radio Link Quality

We assume that the power allocations $\{P_{B,j}^* \mid j = 0, 1, \dots, J\}$ are determined in a heuristic manner, as given by (14). Then, *Proposition 2* below serves as the basis to perform the rate allocation among the mobiles in cell j (tagged cell) so that their SIR requirements are satisfied.

Proposition 2: Given the power allocation $P_{B,j}^*$, rate allocation to the mobiles in cell j can be performed in an ascending order of the *weighted* effective interference factor $\tilde{\mu}_i^{(j)} \triangleq (2^{\kappa_q} \mu_i^{(j)})$, $i \in I_q^{(j)}$ by using the following inequality:

$$\sum_{q=1}^Q 2^{\kappa_q} \left(\sum_{i \in I_q^{(j)}} m_i^{(j)} \mu_i^{(j)} \right) \leq \frac{N}{(\text{SIR})_o} \left(1 - \frac{P_c}{P_{B,j}^*} \right) \triangleq \gamma^{(j)}. \quad (15)$$

Proof of Proposition 2: Multiplying (13) by $m_i^{(j)}$, summing up for $i = 1, 2, \dots, g_j$ and using (2) gives

$$N(P_{B,j}^* - P_c) = \sum_{q=1}^Q 2^{\kappa_q} \left(\sum_{i \in I_q^{(j)}} m_i^{(j)} \mu_i^{(j)} \right) P_{B,j}^* \cdot (\text{SIR})_{o,d} \quad (16)$$

where the set $\{1, 2, \dots, g_j\}$ has been partitioned into the subsets $\{I_q^{(j)} \mid q = 1, 2, \dots, Q\}$. Then, using the inequality $(\text{SIR})_{o,d} \geq (\text{SIR})_o$ in (16) results in (15). ■

The power allocation $P_{b,i}^{(j)}$ at basic rate can be determined from the inequality in (17) below which is derived from (6) using the fact that $(\text{SIR})_{o,i}^{(j)} \geq 2^{\kappa_q} (\text{SIR})_o = (\text{SIR})_{o,q}$ for $i \in I_q^{(j)}$.

$$P_{b,i}^{(j)} \geq \frac{1}{N} \left(2^{\kappa_q} \mu_i^{(j)} \right) P_{B,j}^* \cdot (\text{SIR})_o. \quad (17)$$

Since the rate and power allocation should be such that the total power budget is met [as in (18)], in case the power constraint is violated, the rate allocation in (15) will need to be adjusted so that the power allocation becomes feasible within the total power budget

$$\sum_{i=1}^{g_j} m_i^{(j)} P_{b,i}^{(j)} \leq P_{B,j}^* - P_c. \quad (18)$$

This suboptimal rate and power allocation depends on the total power budget $P_{B,j}^*$ which would vary according to the traffic distribution (i.e., number of users and the corresponding SIR requirements) across the $(J + 1)$ cells.

1) *Uniform Traffic Load:* In this case, we assume $g_j = G$ and $n_q^{(j)} = n_q$ for all j, q . Therefore, total power budget $P_{B,j}^* = P_B$ in (14) and $\gamma = \gamma^{(j)}$ for all j . The following is the procedure for joint rate and power allocation in cell j .

- 1) Sort the mobiles in the ascending order of $\tilde{\mu}_i^{(j)}$.
- 2) For the first mobile in the list, calculate the power allocation at the basic rate as $P_{b,i}^{(j)} = \tilde{\mu}_i^{(j)} P_B (\text{SIR})_o / N$ and allocate the maximum possible rate to this mobile as far as

$$\sum_{i=1}^G m_i^{(j)} \tilde{\mu}_i^{(j)} \leq \gamma \quad \text{and} \quad \sum_{i=1}^G m_i^{(j)} P_{b,i}^{(j)} \leq P_B - P_c.$$

- 3) Repeat step (2) for the second mobile in the list, and so on.

Note that if there is a certain constraint on the rate, namely, $m_i^{(j)} \geq m_q$ for $i \in I_q^{(j)}$, then the rate allocation in step (2) can be easily modified to accommodate the rate constraint along with the power and the multiple SIR constraints.

2) *Nonuniform Traffic Load:* The power budget in this case should be different from cell to cell depending on the traffic distribution across the $(J + 1)$ cells. Given $P_{B,j}^*$, g_j , and $\gamma^{(j)}$, the rate and power allocation is performed in the same way as in the uniform traffic load case.

3) *Complexity:* Since the suboptimal rate and power allocation is performed on a per-cell basis (rather than on a joint-cell basis as in the optimal and near-optimal cases), it does not require the radio network controller (RNC) to inform the base station of the intercell factors corresponding to the mobiles in the other cells during each adaptation interval. The time complexity of the rate and power allocation in this case is of $O(\varphi \cdot g_j)$ in cell j .

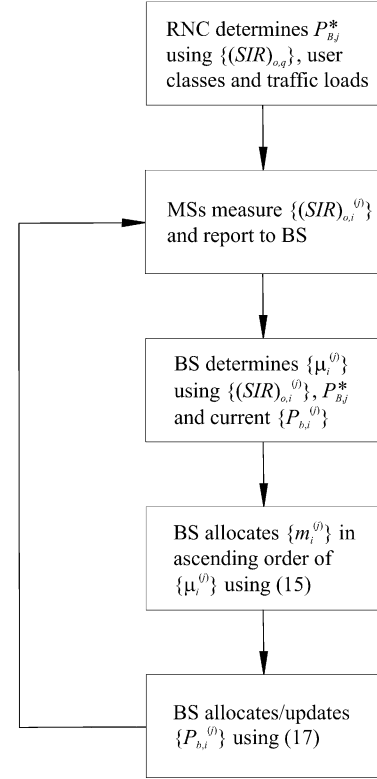


Fig. 1. Flow diagram for the *suboptimal* single-cell rate and power allocation method.

4) *Implementation Issue:* A flow diagram for the suboptimal rate and power allocation method is shown in Fig. 1. Based on the link quality estimates $\{(\text{SIR})_{o,i}^{(j)}\}$, the proposed dynamic joint rate and power adaptation scheme can be implemented in a mobile-assisted and base station-controlled manner. Within the European Telecommunications Standards Institute (ETSI) WCDMA power control framework, such a scheme would not cost extra overhead.

5) *Comparison:* A comparison among the three approaches for dynamic rate and power adaptation is shown in Table II.

B. Dynamic Link Adaptation With Priority

In case of radio link quality-based dynamic link adaptation based on (15), (17), and (18) as described earlier, higher transmission rates will most likely be allocated to a few mobiles with favorable radio link conditions in terms of the weighted effective interference factor $\tilde{\mu}_i^{(j)}$. Again, as is evident from (15), due to rate allocation based on $\tilde{\mu}_i^{(j)} = (2^{\kappa_q} \mu_i^{(j)})$ mobiles with higher SIR requirements are more likely to experience unfairness in terms of sum-rate throughput. The essence is, the weighted effective interference-based rate allocation prevents us from allocating the rate resource according to the individual user requirement. For example, sometimes mobiles with more stringent delay requirements may need to be allocated higher transmission rates even though the corresponding radio link qualities are not very favorable.

For this reason, a dynamic link adaptation scheme is developed which integrates radio link quality-based rate and power allocation with individual user requirement-based (or priority-based) rate allocation in a flexible framework. In addition to providing QoS differentiation among the different service classes

TABLE II
COMPARISON AMONG THE DYNAMIC RATE AND POWER ALLOCATION METHODS

Optimal	Near-optimal	Suboptimal
Joint-cell rate/power alloc.	Joint-cell rate/power alloc.	Single-cell rate/power alloc.
Optimal solutions on $\{P_{B,j}\}$ and $\{m_i^{(j)}\}$ by solving $(J+1)$ equations in (10)	Near-optimal solutions on $\{P_{B,j}\}$ and $\{m_i^{(j)}\}$ by solving $(J+1)$ equations in (10)	–
Rate alloc. in exhaustive manner	Rate alloc. in ascending order of $\{\tilde{\mu}_i^{(j)} \mid i = 1, \dots, g_j; j = 0, \dots, J\}$	Rate alloc. in ascending order of $\{\tilde{\mu}_i^{(j)} \mid i = 1, \dots, g_j\}$, given cell j
Exponential complexity of the order $\sim \varphi \sum_{j=0}^J g_j$	Complexity of the order $\sim \varphi \cdot \sum_{j=0}^J g_j \cdot (J+1)^3$	Complexity of the order $\sim \varphi \cdot g_j$
–	Heuristic per-cell power alloc. $\{P_{B,j}^*\}$ using (14) to determine $\{\mu_i^{(j)}\}$	Heuristic per-cell power alloc. $P_{B,j}^*$ using (14) to determine $\{\mu_i^{(j)}\}$, $\{m_i^{(j)}\}$ and $\{P_{b,i}^{(j)}\}$
Need to estimate $\{\eta_{j'/j}(i) \mid i = 1, \dots, g_j; j' = 0, \dots, J\}$ ($j' \neq j$) in (3)	Need to estimate $\{\eta_{j'/j}(i) \mid i = 1, \dots, g_j; j' = 0, \dots, J\}$ ($j' \neq j$) in (3)	$\{\mu_i^{(j)}\}$ to be estimated by periodic SIR measurements in (6)

in terms of SIR, such a scheme essentially enables to provide flexible service differentiation in terms of other QoS parameters such as delay. This is achieved at the cost of loss in the sum-rate throughput in a cell.

In the proposed scheme, the procedure for allocating transmission rates to the mobiles in cell j in the proposed scheme is shown in the following.

- 1) Sort the mobiles in the ascending order of $\tilde{\mu}_i^{(j)}$.
- 2) For the first mobile in the list, calculate the power allocation at the basic rate as $P_{b,i}^{(j)} = \tilde{\mu}_i^{(j)} P_{B,j}^*(\text{SIR})_o/N$ and allocate the maximum possible rate to this mobile as far as (19) is satisfied with $m_i^{(j)} \leq \varphi$ and $\lfloor m_i^{(j)} \cdot \alpha^{-l_q} \rfloor$ being the allocated rate ($\lfloor x \rfloor$ denotes the largest integer not exceeding x) and

$$\sum_{i=1}^{g_j} \left\lfloor m_i^{(j)} \cdot \alpha^{-l_q} \right\rfloor \cdot P_{b,i}^{(j)} \leq P_{B,j}^* - P_c.$$

Here, α and l_q are the rate control and priority control parameters, respectively.

- 3) Repeat step (2) for the second mobile in the list, and so on.

$$\sum_{q=1}^Q 2^{\kappa_q} \left(\sum_{i \in \mathcal{I}_q^{(j)}} \left\lfloor m_i^{(j)} \cdot \alpha^{-l_q} \right\rfloor \cdot \mu_i^{(j)} \right) \leq \gamma^{(j)}$$

$$0 < \alpha \leq 1.0, \quad l_q \leq 0, \quad q = 1, 2, \dots, Q. \quad (19)$$

With $\alpha = 1.0$, rate adaptation in this case is based only on radio link conditions where mobiles with higher SIR requirements are likely to be penalized in terms of average-rate throughput.⁵ As the value of the rate control parameter α decreases, fairness (in terms of average-rate throughput) among users in the classes with different requirements would be improved while the sum-rate throughput (or equivalently, channel utilization) would be degraded. Therefore, by controlling α , the desired tradeoff between fairness and efficiency could be achieved.

Again, together with α , the priority control parameter l_q can be varied to control the transmission rate allocation among

⁵For the i th mobile in cell j , this is the average number of radio link level frames transmitted per frame-time under the corresponding SIR constraint and is denoted by $E(m_i^{(j)})$.

mobiles in the different service classes. For a certain value of α , as l_q increases/decreases the transmission rates allocated to the mobiles in the service class q increase/decrease. Therefore, if the users corresponding to the service class with higher SIR requirements have tighter delay requirements (e.g., real-time video users), better transmission rates can be allocated to the corresponding mobiles by decreasing/increasing the value of the priority control parameter for the service class(es) with lower/higher SIR requirements. In any case, the minimum SIR requirements in terms of κ_q for all the service classes as given in (9) are guaranteed. Note that, the rate and the priority control parameters can be adjusted on a frame-by-frame basis depending on the radio link conditions and thereby a flexible dynamic rate and power allocation can be achieved.

Note that, the impacts of variations in α and l_q on the average-rate throughput $E(m_i^{(j)})$ may not be quite observable unless the restriction $m_i^{(j)} \leq \varphi$ is imposed in (19). In other words, using the constraint $\lfloor m_i^{(j)} \cdot \alpha^{-l_q} \rfloor \leq \varphi$ (instead of $m_i^{(j)} \leq \varphi$) would make it more difficult to achieve the QoS differentiation among the mobiles over a wide range of average-rate throughput.

V. ANALYSIS OF THE AVERAGE SUM-RATE THROUGHPUT

In this section, the sum-rate throughput is evaluated for the suboptimal rate allocation [based on (15)] using the average value of the effective interference factor $\mu_i^{(j)}$ in (5) for random user mobility. We assume a hexagonal cell layout with normalized cell radius of unity and uniform distribution of mobiles within each cell.

Since the long-term channel gain $L_j(j, i)$ corresponding to mobile i in cell j (tagged cell) should be greater than $L_{j'}(j, i)$ for all other cells, the average value of the effective interference factor $\mathbf{E}\{\mu_i^{(j)}\}$ can be expressed by

$$\mathbf{E}\{\mu_i^{(j)}\} = \left[(1 - \nu) + \sum_{j' \neq j} \beta_{j'/j} \cdot \mathbf{E}\left\{ \frac{\zeta_i^{(j')} L_{j'}(j, i)}{\zeta_i^{(j)} L_j(j, i)} \mid L_{j'}(j, i) < L_j(j, i) \right\} \right]. \quad (20)$$

Due to the independence assumption on short-term fading with $\mathbf{E}\{\zeta_i^{(j')}\} = 1$ for all j' , (20) can be written as

$$\mathbf{E}\left\{\mu_i^{(j)}\right\} = \left[(1 - \nu) + \sum_{j' \neq j} \beta_{j'/j} \cdot \mathbf{E}\left\{ \frac{L_{j'}(j, i)}{L_j(j, i)} \mid L_{j'}(j, i) < L_j(j, i) \right\} \right]. \quad (21)$$

By referring to [9] and [12], the expected value can be evaluated as

$$\mathbf{E}\left\{\mu_i^{(j)}\right\} = \left[(1 - \nu) + \sum_{\substack{(\pm k, \pm l) \\ k+l=2n}} \beta_{(k,l)/j} \int \int f(k, l) \cdot \left(\frac{u^2 + v^2}{(u + \sqrt{3}k/2)^2 + (v + 3l/2)^2} \right)^{\delta/2} \cdot \left(\frac{2}{3\sqrt{3}} \right) du dv \right] \quad (22)$$

where the integral is evaluated numerically over the area of center cell j , $\beta_{(k,l)/j} = P_{B,(k,l)}/P_{B,j}$ for $(k, l) \equiv j' \neq j$, and

$$f(k, l) = \exp[(\sigma \ln 10/10)^2] \left\{ 1 - Q \left[\frac{5\delta}{\sqrt{2\sigma^2}} \right] \cdot \log_{10} \left(\frac{(u + \sqrt{3}k/2)^2 + (v + 3l/2)^2}{u^2 + v^2} \right) - \sqrt{2\sigma^2} \frac{\ln 10}{10} \right\} \quad (23)$$

where σ is the standard deviation (dB) of the random variable $\xi_{i,j}$ in (4), and $Q(x) = 1/\sqrt{2\pi} \int_x^\infty e^{-y^2/2} dy$.

Based on the average value $\bar{\mu}_j = \mathbf{E}\{\mu_i^{(j)}\}$, the *average weighted effective interference factor* $\tilde{\mu}_i^{(j)} = (2^{\kappa_q} \bar{\mu}_j) \triangleq \tilde{\mu}_q^{(j)}$ can be determined (where $i \in I_q^{(j)}$ and $q = 1, 2, \dots, Q$). In fact, the *average weighted interference factor* $\tilde{\mu}_q^{(j)}$ for class q is largely affected by the corresponding SIR requirement κ_q since the average value of the interference factor $\mu_i^{(j)}$ would not be much different for all the mobiles under random mobility assumption.

Based on (15), when the suboptimal rate allocation is performed in an ascending order of the interference factor $\tilde{\mu}_q^{(j)}$, mobiles in the service class with lower κ_q are more likely to be allocated transmission rates. That is, with $\kappa_1 \leq \kappa_2 \leq \dots \leq \kappa_Q$, the suboptimal rate allocation is performed in an increasing order of q , i.e., $q = 1, 2, \dots, Q$ until the inequality in (15) is satisfied. In such a case, the following inequalities hold ($0 \leq s \leq Q - 1$):

$$\sum_{q=1}^s 2^{\kappa_q} n_q^{(j)} [\varphi \cdot \alpha^{-l_q}] \leq \bar{\mu}_j^{-1} \gamma^{(j)} \quad (24)$$

$$\sum_{q=1}^{s+1} 2^{\kappa_q} n_q^{(j)} [\varphi \cdot \alpha^{-l_q}] > \bar{\mu}_j^{-1} \gamma^{(j)} \quad (25)$$

where the maximum allowable rate $m_i^{(j)} = \varphi$ is dynamically adjusted depending on the rate control parameter α and the priority control parameter l_q . Note that, if $s = Q$ in (24), all the mobiles in all the service classes can be allocated transmission rates (i.e., there is no congestion).

Now, the sum-rate throughput in the target cell j , denoted by C_j , can be bounded by

$$\sum_{q=1}^s n_q^{(j)} [\varphi \cdot \alpha^{-l_q}] \leq C_j < \sum_{q=1}^{s+1} n_q^{(j)} [\varphi \cdot \alpha^{-l_q}] \quad (26)$$

where the value of s can be found from (24) and (25). From (24), we can find the largest $m < \varphi$ such that

$$2^{\kappa_{s+1}} \Delta_{s+1}^{(j)} \leq \bar{\mu}_j^{-1} \gamma^{(j)} - \sum_{q=1}^s 2^{\kappa_q} n_q^{(j)} [\varphi \cdot \alpha^{-l_q}] \quad (27)$$

where $\Delta_{s+1}^{(j)} = \sum_{i \in I_{s+1}^{(j)}} [m_i^{(j)} \cdot \alpha^{-l_{s+1}}]$.

Since this upper bound would be tight due to the suboptimal rate allocation, where the rate allocation continues as far as there is any residual rate resource, the sum-rate throughput will closely converge to the bound. Therefore, the average-sense sum-rate throughput in cell j , \bar{C}_j , can be approximated to

$$\bar{C}_j \cong \sum_{q=1}^s n_q^{(j)} [\varphi \cdot \alpha^{-l_q}] + \Delta_{s+1}^{(j)}. \quad (28)$$

With the previous formulation, where the radio link condition is taken into account in the average sense by $\bar{\mu}_j$, the radio link level performance (in terms of average sum-rate throughput in cell j , \bar{C}_j) under dynamic rate adaptation can be investigated under different traffic distributions (as characterized by $\{n_q^{(j)}\}$) when the mobiles have different SIR requirements (as specified by $\{\kappa_q\}$). Furthermore, the parameter s measures indirectly fairness in throughput among users with different SIR requirements. For instance, as s increases, the fairness improves since the rate allocation becomes more even among users in the different service classes.

Let us consider a time-varying traffic distribution where the number of users in each service class has Poisson distribution so that the value of the parameter $n_q^{(j)}$ is given by

$$\Pr [n_q^{(j)} = k_q] = e^{-\lambda_q} \frac{\lambda_q^{k_q}}{k_q!} \quad k_q = 0, 1, \dots \quad (29)$$

where λ_q denotes the average number of users belonging to service class $q = 1, 2, \dots, Q$ during a frame-time and $\{n_q^{(j)} \mid q = 1, 2, \dots, Q\}$ are mutually independent.

With the Poisson traffic model, the fairness factor \bar{s} may be defined and derived by

$$\begin{aligned} \bar{s} &\triangleq \mathbf{E}\{s(k_1, \dots, k_Q)\} \\ &= \sum_{k_1 \geq 0} \dots \sum_{k_Q \geq 0} s(k_1, \dots, k_Q) \left(\prod_{q=1}^Q e^{-\lambda_q} \frac{\lambda_q^{k_q}}{k_q!} \right) \end{aligned} \quad (30)$$

where $s = s(k_1, \dots, k_Q)$ is found in (24) and (25) by letting $n_q^{(j)} = k_q$ for all q . Therefore, by observing \bar{s} , the performance behavior in terms of the fairness in rate allocation among different service classes can be analyzed under varying traffic distribution.

VI. SIMULATION MODEL, RESULTS AND DISCUSSIONS

A. Models for Micro-Mobility, Shadowing and Multipath Fading

We consider two micro-mobility models, namely, the random mobility model and the directional mobility model. In the former case, the location of each mobile user during each frame-time is chosen randomly inside the target cell and the effect of shadowing at different locations is assumed to be uncorrelated. In the latter case, we assume a directional random walk model [13] where the mobile users travel from a starting point to a destination in a series of statistically independent discrete steps. In this case, the effect of shadowing at the different locations is assumed to be correlated. For each step, the angular deviation (θ) of the travel direction from the *principal direction*⁶ has the probability density function $f(\theta)$ given by

$$f(\theta) = \begin{cases} \frac{A_\theta}{2[1 + A_\theta^2 \theta^2] \tan^{-1}(A_\theta \pi)}, & -\pi \leq \theta \leq \pi \\ 0, & \text{otherwise.} \end{cases} \quad (31)$$

The parameter A_θ controls how close the travel direction is to the principal direction. If a mobile user travels in a forward direction with probability 0.95, the corresponding value for A_θ is 4.2 [13]. We assume that all the mobile users have a constant speed of v and that for each user the successive points are separated (in time) by one frame-time.

The correlated shadowing is modeled as a Gaussian white noise process, filtered through a first degree low-pass filter as follows [14]:

$$\omega_{k+1}(\text{dB}) = a \times \omega_k(\text{dB}) + (1 - a) \times c_k \quad (32)$$

where $\omega_k(\text{dB})$ is the mean envelope level or mean square-envelope level (in dB) that is experienced at location k , a is the correlation coefficient given by $a = \varepsilon_D^{vT_s/D}$, and c_k is a zero-mean Gaussian random variable with variance $\tilde{\sigma}^2$. Here, $\tilde{\sigma}^2 = (1 + a)/(1 - a)\sigma^2$, with σ^2 being the variance of log-normal shadowing. The parameter ε_D is the correlation between two points separated by distance D and T_s is the sampling interval (which is assumed to be equal to the frame-time T in this paper).

Multipath fading is assumed to be independently varying. In the random mobility case, an L -path ($L = 3$) Rayleigh-fading channel with uncorrelated scattering and equal average path power is assumed. Multipath fading with unequal average path power is assumed for the directional mobility with correlated shadowing case and the parameters are based on the vehicular-B model [15] for macro-cell.

B. Performance Metrics and Simulation Methodology

To evaluate the performances of the dynamic rate and power adaptation schemes by computer simulation, we determine the average transmission rate per frame-time for the mobiles in the target cell (i.e., average-rate throughput for the i th mobile in cell j , $E(m_i^{(j)})$) and also the average transmission rate per mobile per frame-time (i.e., $E(m_i)$) over all the mobiles in all the cells.

The values of some of the system parameters used for obtaining the results presented in this paper are listed in Table III.

⁶At any point on the travel path, the line joining the point to the destination defines the principal direction.

TABLE III
SYSTEM PARAMETERS

Parameter	Value
Frame-time, T	10 ms
Chip sequence length, N	128
Path loss exponent, δ	4.0
Standard dev. of shadow fading, σ	8 dB
ν	0.2
P_c/P_B	0.2
$(SIR)_o$, dB	2, 3, 4, 5, 6, 7, 8
D	100 m
ε_D	0.1
A_θ	4.2
v	20, 50, 80 km/hr
φ	3, 8
J	2, 6

Three classes of users (i.e., $q = 1, 2, 3$) with different SIR requirements (e.g., $2^{k_q} = 1, 2, 3$, $2^{k_q} = 1, 1.26, 2$) are considered in each cell. For example, with $2^{k_q} = 1, 1.26, 2$, and $(SIR)_o = 3$ dB, the minimum SIR requirements are 3, 4, and 6 dB for $q = 1, q = 2$, and $q = 3$, respectively. Seven cells (i.e., $J = 6$) are considered in a hexagonal cell-layout and ‘‘cell 0’’ is assumed to be the tagged cell. The number of users in each of the cells is assumed to be 20 (i.e., $g_0 = g_1 = \dots = g_6 = 20$). The service classes for the mobiles in the tagged cell are as follows: $I_1^{(0)} = \{0, 1, \dots, 6\}$, $I_2^{(0)} = \{7, 8, \dots, 13\}$, $I_3^{(0)} = \{14, 15, \dots, 19\}$.

Since, for the system configuration finding the optimal rate and power allocation from (10) by using exhaustive search is infeasible, we observe the throughput performance of the optimal scheme for a smaller system configuration with three cells and three users per cell (i.e., $g_0 = g_1 = g_2 = 3$).

The locations of the mobiles in the tagged cell are generated randomly during each iteration and the number of iterations used for collecting the results is sufficiently large (e.g., 10^5). In the case of directional mobility model with correlated shadowing, during each iteration, the initial locations of the mobiles are generated randomly within the target cell and the successive locations are generated by using (31) based on the mobile speed (v) and the length of the adaptation interval (or frame-time, T). The destination point is assumed to be located in the tagged cell and while generating the successive mobile locations, it is ensured that the locations are within the tagged cell.

In each case, simulations are performed to obtain the maximum average-rate throughput.⁷ For this, the intercell interference factor $\eta_{j' / j}(i)$ is calculated using (3) to evaluate the effective interference factor $\mu_i^{(j)}$ in (5). In this case, $L_{j'}(j, i) > L_j(j, i)$ for all j' (i.e., the base station in the tagged cell is selected as the serving base station). The values of $L_{j'}(j, i)$ and $L_j(j, i)$, which account for the long-term fading, are assumed to be constant over a frame-time (T).

The values of $\zeta_i^{(j')}$ and $\zeta_i^{(j)}$, which account for the short-term fading in (3), are assumed to be constant only over a fraction of the frame-time Δt , where $T = K \Delta t$. Therefore, the value of

⁷The average-rate throughput may fall below this maximum value in the soft-handoff case due to increased $\eta_{j' / j}(i)$.

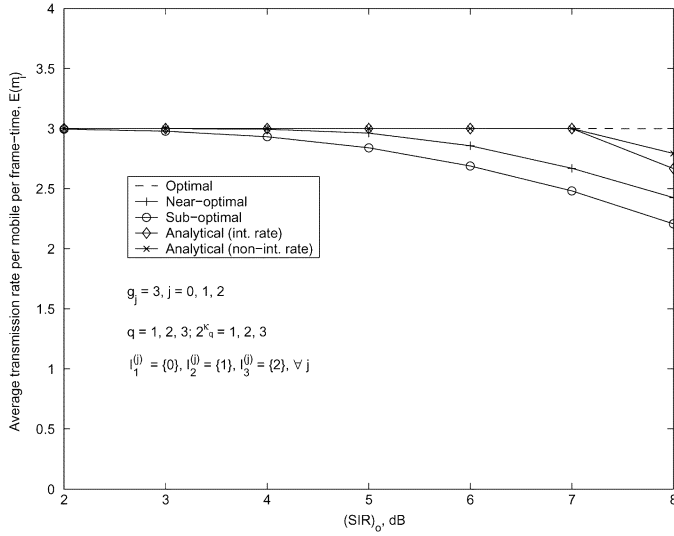


Fig. 2. Average transmission rate per mobile per frame-time for optimal, near-optimal, and suboptimal dynamic rate adaptation (for the random mobility model) when $\varphi = 3$.

$\eta_{j'} / j(i)$ over a frame-time is calculated by using the average of the K independent values of $\zeta_i^{(j')} / \zeta_i^{(j)}$. The value of K is assumed to be 16 in this paper.

In the case of near-optimal rate adaptation, the rate allocation is performed in an ascending order of $\tilde{\mu}_i^{(j)}$ by allocating the maximum allowable rate as far as the allocated rates satisfy (10) and until the sum of the transmission rates is maximized. The power allocations to estimate the values of $\mu_i^{(j)}$ are determined using (14) for both the near-optimal and the suboptimal rate adaptation schemes.

To evaluate the average sum-rate throughput using the proposed analytical approach, both the integer and the noninteger rate allocations are considered. In the former case, the integer parts of $\varphi \cdot \alpha^{-l_q}$ and $m \cdot \alpha^{-l_{s+1}}$ are considered while evaluating \bar{C}_j , the average sum-rate throughput in cell j , by using (28).

C. Results and Discussions

1) *Optimal, Near-Optimal, and Suboptimal Rate Adaptation:* Typical results on the average transmission rate per mobile per frame-time (average-rate throughput) under optimal, near-optimal, and suboptimal rate adaptation schemes are presented in Figs. 2 and 3. The average-rate throughput for the random mobility case found from analytical approximation is also plotted in the same figures for comparison.

As is evident, the throughput performance of all the three schemes are fairly close over a range of values of $(SIR)_o$. The throughput performance for the suboptimal case is fairly close to that of the near-optimal case. Depending on the value of $(SIR)_o$ the near-optimal scheme may provide slightly better throughput than the suboptimal case. However, from the cost and complexity viewpoint the use of the near-optimal scheme may not be preferable to the suboptimal scheme.

The analytical results on average-rate throughput in Fig. 2 are observed to upper bound the simulation results, which is due to the more optimistic average-sense approximation of the interference factor (note that, we consider a smaller system configuration consisting of only three cells with three users per cell in

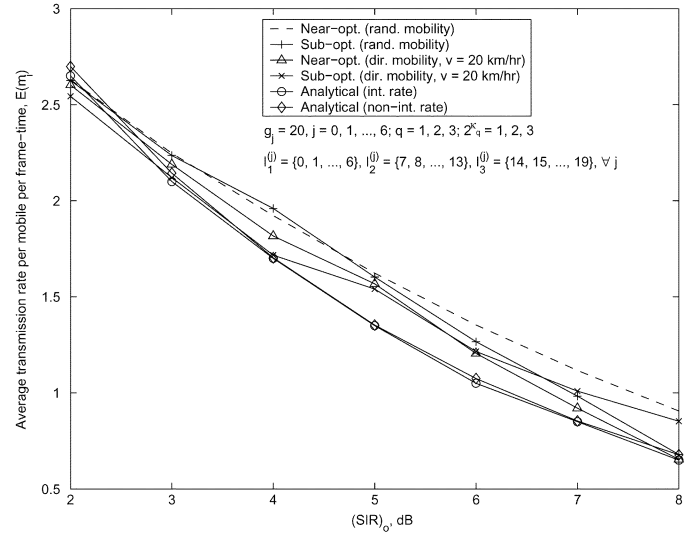


Fig. 3. Average transmission rate per mobile per frame-time for near-optimal and suboptimal dynamic rate adaptation when $\varphi = 8$.

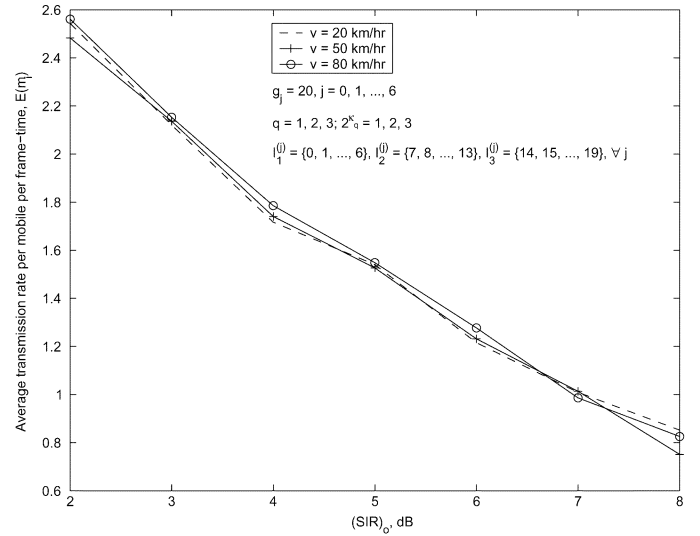


Fig. 4. Average transmission rate per mobile per frame-time under suboptimal dynamic rate adaptation for the directional mobility model when $\varphi = 8$.

this case). As the number of users increases, the multiuser diversity will be increased so that in each cell the user with the best channel condition will be allocated most of the rate resource $\gamma^{(j)}$ in (15), resulting in a nonlinear rate allocation with respect to the channel condition. However, the average-sense approximation is based on the rate allocation in proportion to the mean interference factor. As a result, for a larger system configuration (e.g., in Fig. 3), the analytical results will lower bound the throughput performance of the suboptimal scheme.

Simulation results show that, for the assumed system parameters, variation in terminal speed v (e.g., $v = 20, 50, 80$ km/h) does not have significant impact on the average-rate throughput (Fig. 4). Although correlated shadowing impacts the channel conditions of all the mobiles, for the radio link quality-based rate adaptation, the transmission rate allocation is done only for a subset of the mobiles (with better channel conditions) during an adaptation interval. This makes the impact of terminal velocity on the average-rate throughput not much significant in our model. However, the impact of imperfect power control on

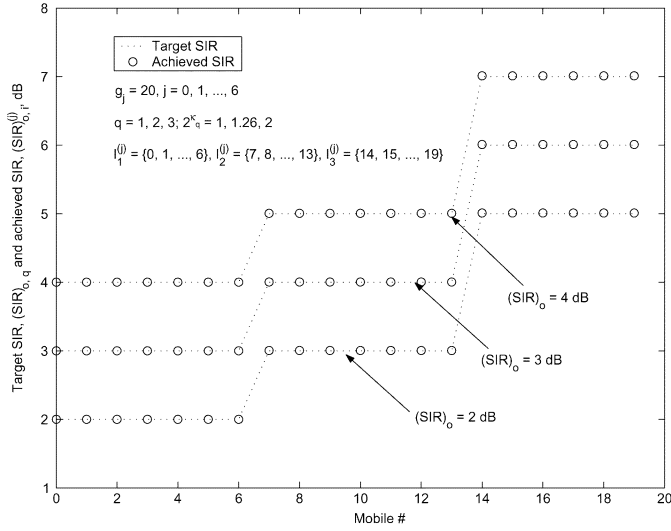


Fig. 5. Target SIR and achieved SIR for the mobiles in the tagged cell (for the random mobility model) when $\varphi = 8$.

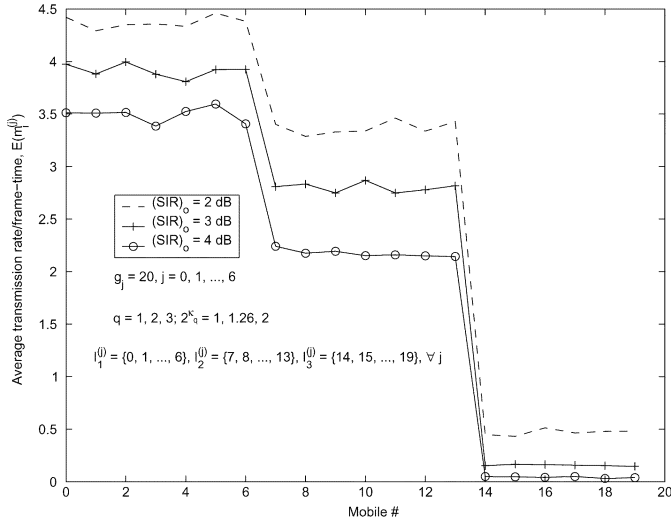


Fig. 6. Impact of $(SIR)_o$ on average transmission rate per frame-time for the mobiles in the tagged cell (for the random mobility model) when $\varphi = 8$.

sum-rate throughput, when considered, would be worse for high-mobility users compared to that for the low-mobility users.

2) *Average-Rate Throughput and Achieved SIR With Suboptimal Rate Adaptation:* The achieved signal-to-interference ratios for the different mobiles in the tagged cell closely follow the corresponding target SIRs (Fig. 5). Similar results are obtained for the mobiles in other cells. Since the value of $\gamma^{(j)}$ in (15) decreases with increasing $(SIR)_o$, the average transmission rate per frame-time for the different mobiles decreases with increasing $(SIR)_o$ (Fig. 6). With radio link quality-based rate allocation, mobiles with higher SIR requirements are allocated lower rates due to larger weighted effective interference factor $\tilde{\mu}_i^{(j)}$.

For the directional mobility with correlated shadowing case, short-term unfairness in rate allocation may result due to the differences among the achieved average transmission rate per frame-time for the different mobiles in the same service class

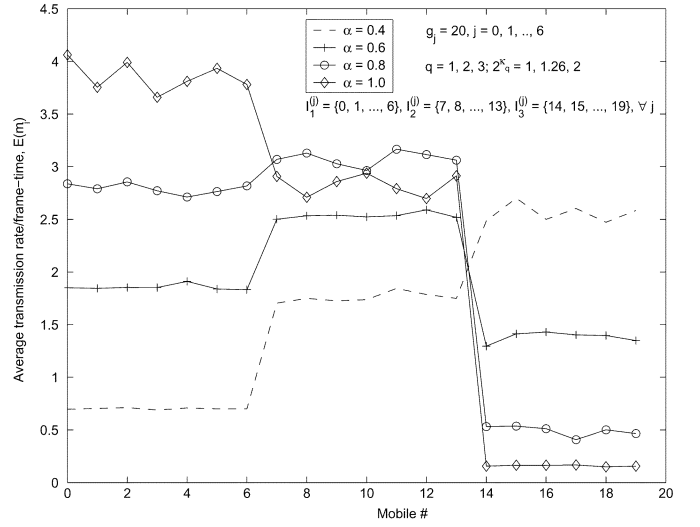


Fig. 7. Impact of rate control parameter α on average transmission rate per frame-time for the mobiles in the tagged cell (for the random mobility model) when $\varphi = 8$.

(which is caused by variations in the channel condition due to correlated shadowing).

3) *Impact of Rate and Priority Control Parameters:* When the value of the rate control parameter α is 1.0, the rate adaptation is based on radio link condition only and this may cause the average transmission rate per frame-time for the mobiles with higher SIR requirements to drop significantly. This problem may be alleviated by using $\alpha < 1.0$. The amount of improvement in the average-rate throughputs for the mobiles with higher SIR requirements would depend on the distribution of the SIR requirements among the users. As the value of the rate control parameter α decreases, the average transmission rate per frame-time for mobiles with lower/higher SIR requirements decreases/increases (Fig. 7). For the assumed distribution of SIR requirements, the average transmission rate per frame-time for the mobiles with higher SIR requirements improves remarkably with decreasing α .

The priority control parameter l_q and the rate control parameter α may be properly selected depending on the user requirements in the corresponding service classes. For example, the service class with higher SIR requirement may be assigned the priority level $l_q = 0$ while the service class with lower SIR requirement may be assigned the priority level $l_q < 0$ so that the transmission rate allocation becomes more even among users in the different service classes (as observable from $E(m_i)$ for $\{l_1 = 0, l_2 = -1, l_3 = -2\}$ and $\{l_1 = -2, l_2 = -1, l_3 = 0\}$ in Fig. 8). As the priority control parameter l_q for the service class with higher SIR requirement is increased, the average transmission rate per frame-time for the mobiles in that service class increases (Fig. 8). Again, the reverse effect can be produced by adjusting l_q and α , for example, when the channel conditions for the users in the service class with higher SIR requirement deteriorate.

The average transmission rate per mobile per frame-time (or average-rate throughput) decreases with increased priority (larger l_q) to mobiles with higher SIR requirements (or equivalently, lower priority (smaller l_q) to mobiles with lower SIR requirements). For example, the average rate throughput with

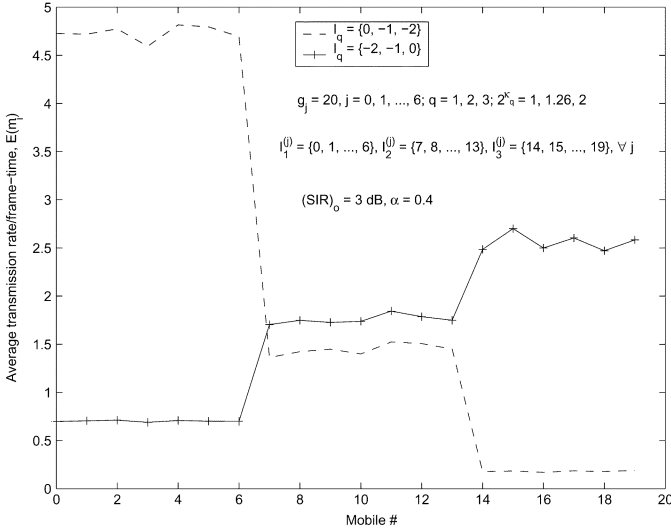


Fig. 8. Impact of priority control parameters on average transmission rate per frame-time for the mobiles in the tagged cell (for the *random* mobility model) when $\varphi = 8$.

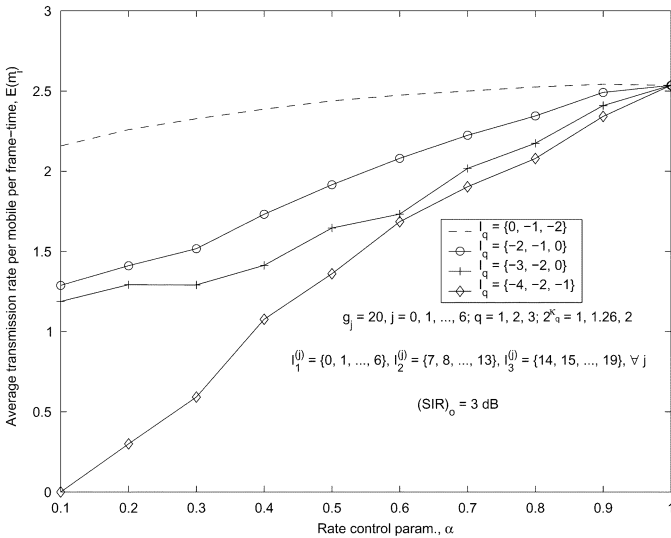


Fig. 9. Impact of priority control parameters on average-rate throughput (for the *random* mobility model) when $\varphi = 8$.

$l_1 = -2$ is smaller compared to that for $l_1 = 0$ (Fig. 9). The desired tradeoff between the average-rate throughput and the fairness in rate allocation among mobiles in the different service classes can be obtained by adjusting both the rate control parameter α and the priority control parameter l_q appropriately and thereby a flexible combined link quality-based and priority-based rate adaptation can be achieved.

The average-rate throughputs found from analytical approximation follow the simulation results more or less closely (Fig. 10). The rate and priority control parameters for an acceptable region of operation can, therefore, be estimated based on the analytical approximations. The analytical results on the average-rate throughput are observed to act as lower bound. The analytical approximation on the average-rate throughput is based on the average interference factor [in (24) and (25)] and the assumption that the rate allocation is performed in an ascending order of κ_q for all the mobiles in the corresponding service classes. Even though the approximation is based on the

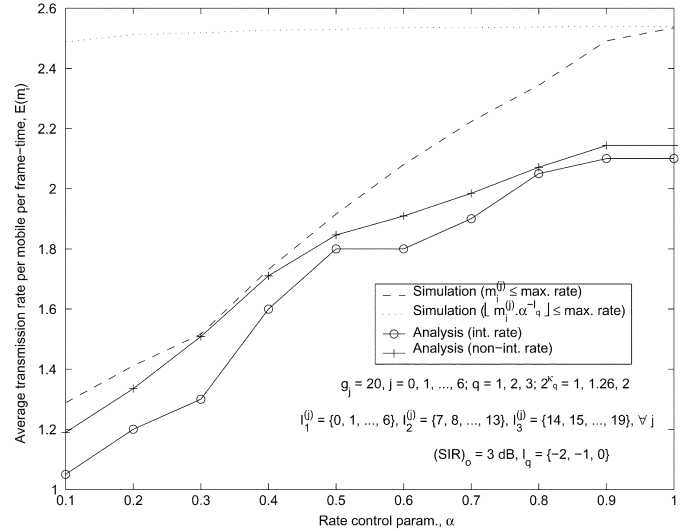


Fig. 10. Comparison among the simulation and the analytical results on average-rate throughput (for the *random* mobility model) when $\varphi = 8$.

fact that for small α and/or l_q , rate allocations to the mobiles in service classes with smaller l_q may become zero and rates are mostly allocated to mobiles in the service class with higher l_q , the average interference factor used in the approximation may become much larger compared to the interference factors that mobiles in the service class with higher l_q experience from frame-time to frame-time. Again, due to the assumption that the rate allocation is performed in an ascending order of κ_q , the (negative) effect of higher weighted interference factor $\tilde{\mu}_i^{(j)}$ (due to mobiles with higher SIR requirements) on average-rate throughput is somewhat more pronounced in the analytical approximations.

Note that, for dynamic link adaptation with priority the constraint $m_i^{(j)} \leq \varphi$ in (19) makes the variations in the rate and priority control parameters effective in controlling the average-rate throughput among the users in the different classes (as discussed in Section IV-B). This is also illustrated in Fig. 10. Removing this constraint and using the constraint $[m_i^{(j)} \cdot \alpha^{-l_q}] \leq \varphi$ instead may not enable to provide QoS differentiation over a wide range of average-rate throughput as evidenced by the very slowly varying nature of the corresponding curve in Fig. 10.

VII. CONCLUSION

In this paper, a dynamic link adaptation framework is presented for dynamic allocation of transmission rate and power under multiple SIR constraints for downlink transmission in cellular VSF WCDMA networks. Heuristic-based simple suboptimal dynamic rate and power adaptation scheme is proposed to avoid the huge complexity of optimal dynamic link adaptation which is almost infeasible to implement. The concepts of radio link quality-based link adaptation is combined with the user priority-based link adaptation and this would enable to develop a class-based QoS framework for the cellular multirate WCDMA networks. An approach for analytical investigation of the radio link level performance under dynamic link adaptation with multiple SIR constraints is also presented which would be useful for system engineering purposes. The proposed framework can serve as a basis for investigating higher-layer protocol

performance under dynamic radio link adaptation with QoS differentiation in cellular WCDMA networks.

APPENDIX

HEURISTIC DETERMINATION OF $P_{B,j}^*$ IN (14)

In (13), we note that, given $P_{B,j}$ and $(\text{SIR})_{o,d}$, the per-user power allocation at basic rate $P_{b,i}^{(j)}$ is proportional to the factor $2^{\kappa_q} \mu_i^{(j)}$ for $i \in I_q^{(j)}$. Combining this with (2) yields

$$P_{B,j} - P_c = \frac{1}{N} \left[\sum_{i=1}^{g_j} 2^{\kappa_{q_i}} \left(m_i^{(j)} \mu_i^{(j)} \right) \right] P_{B,j} \cdot (\text{SIR})_{o,d} \quad (33)$$

where $i \in I_q^{(j)}$ for $q_i \in \{1, 2, \dots, Q\}$. Since the interference factor $\mu_i^{(j)}$ in (5) cannot be estimated without *a priori* knowledge of the per-cell power allocations $\{P_{B,j}\}$, and also the the rate allocation $m_i^{(j)}$ is inversely proportional to $\mu_i^{(j)}$, while determining $P_{B,j}^*$ we treat the factor $(m_i^{(j)} \mu_i^{(j)})$ to be approximately constant. Therefore, the per-cell power allocation $P_{B,j}$ should be increased in proportion to $\sum_{q=1}^Q 2^{\kappa_q} n_q^{(j)}$ where $n_q^{(j)} = |I_q^{(j)}|$ and $\sum_{q=1}^Q n_q^{(j)} = g_j$. Hence, the per-cell power allocation can be calculated approximately by $P_{B,j}^*$ as in (14) subject to the average power constraint per cell P_B in (8).

REFERENCES

- [1] H. Honkasalo, K. Pehkonen, M. T. Niemi, and A. T. Leino, "WCDMA and WLAN for 3G and beyond," *IEEE Wireless Commun.*, vol. 9, pp. 14–18, Apr. 2002.
- [2] Y. Guo and H. Chaskar, "Class-based quality of service over air interfaces in 4G mobile networks," *IEEE Commun. Mag.*, vol. 40, pp. 132–137, Mar. 2002.
- [3] M. O. Sunay and J. K\"{a}ht\"{a}v\"{a}, "Provision of variable data rates in third generation wideband DS CDMA systems," in *Proc. IEEE Wireless Communications and Networking Conf.*, 1999, pp. 505–509.
- [4] S. A. Jafar and A. Goldsmith, "Optimal rate and power adaptation for multirate CDMA," in *Proc. IEEE Vehicular Technology Conf.*, Fall 2000, pp. 994–1000.
- [5] A. Sampath, P. S. Kumar, and J. M. Holtzman, "Power control and resource management for a multimedia CDMA wireless system," in *Proc. IEEE Int. Symp. Personal, Indoor and Mobile Radio Communications*, Sept. 1995, pp. 21–25.
- [6] S.-J. Oh and K. M. Wasserman, "Adaptive resource allocation in power constrained CDMA mobile networks," in *Proc. IEEE Wireless Communications and Networking Conf.*, Sept. 1999, pp. 510–514.
- [7] D. Ayyagari and A. Ephremides, "Power control based admission algorithms for maximizing throughput in DS-CDMA networks with multimedia traffic," in *Proc. IEEE Wireless Communications and Networking Conf.*, Sept. 1999, pp. 631–635.
- [8] S. Ulukus and L. J. Greenstein, "Throughput maximization in CDMA uplinks using adaptive spreading and power control," in *Proc. IEEE Int. Symp. Spread Spectrum Techniques and Applications*, Sept. 2000, pp. 565–569.
- [9] D. I. Kim, E. Hossain, and V. K. Bhargava, "Downlink joint rate and power allocation in cellular multi-rate WCDMA systems," *IEEE Trans. Wireless Commun.*, vol. 2, pp. 69–80, Jan. 2003.
- [10] Y. Guo and H. Chaskar, "Differentiated services over 3G CDMA air interfaces with location and class-based resource sharing," in *Proc. 3G Wireless*, San Francisco, CA, May 2001.
- [11] J. Postel, *Transmission Control Protocol: Internet*, Sept. 1981. RFC 793.
- [12] K. S. Gilhousen *et al.*, "On the capacity of a cellular CDMA system," *IEEE Trans. Veh. Technol.*, vol. 4, pp. 303–312, May 1991.
- [13] T. K. Kim and C. Leung, "Generalized paging schemes for cellular communications systems," in *Proc. IEEE Pacific Rim Conf. Communications, Computers, and Signal Processing*, Aug. 1999, pp. 217–220.
- [14] M. Gudmundson, "Correlation model for shadow fading in mobile radio systems," *Electron. Lett.*, vol. 27, no. 23, pp. 2145–2146, Nov. 1991.
- [15] *Guidelines for evaluation of radio transmission technologies for IMT-2000*, Rec. ITU-R M.1225, 1997.



Dong In Kim (S'89–M'91–SM'02) received the B.S. and M.S. degrees in electronics engineering from Seoul National University, Seoul, Korea, in 1980 and 1984, respectively, and the M.S. and Ph.D. degrees in electrical engineering from the University of Southern California (USC), Los Angeles, in 1987 and 1990, respectively.

From 1984 to 1985, he was with the Korea Telecom Research Center, Seoul, as a Researcher. From 1986 to 1988, he was a Korean Government Graduate Fellow in the Department of Electrical Engineering, USC. From 1991 to 2002, he was with the University of Seoul, leading the Wireless Communications Research Group. He was a Visiting Professor at University of Victoria, Victoria, BC, Canada, from 1999 to 2000. Since 2002, he has been with Simon Fraser University, Burnaby, BC, where he is an Associate Professor of the School of Engineering Science. He has performed research in the areas of packet radio networks and spread-spectrum systems since 1988. His current research interests include spread-spectrum systems, cellular mobile communications, indoor wireless communications, and wireless multimedia networks.

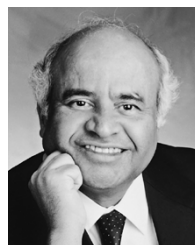
Dr. Kim has served as an Editor of the IEEE JOURNAL ON SELECTED AREAS IN COMMUNICATIONS Wireless Communications Series and also as a Division Editor for the *Journal of Communications and Networks*. He currently serves as an Editor for Spread-Spectrum Transmission and Access for the IEEE TRANSACTIONS ON COMMUNICATIONS and as an Editor for the IEEE TRANSACTIONS ON WIRELESS COMMUNICATIONS.



Ekram Hossain (S'98–M'01) received the B.Sc. and M.Sc. degrees in Computer Science and Engineering from Bangladesh University of Engineering and Technology (BUET), Dhaka, in 1995 and 1997, respectively, and the Ph.D. in electrical engineering from the University of Victoria, Victoria, BC, Canada, in 2000. He was a University of Victoria Fellow and received British Columbia Advanced Systems Institute Graduate Scholarship.

He is an Assistant Professor in the Department of Electrical and Computer Engineering, University of Manitoba, Winnipeg, MB, Canada, where he also leads the Wireless Internet and Packet Radio Network Research Group. His main research interests include radio link control and transport layer protocol design and cross-layer optimization issues for the next-generation wireless data networks.

Dr. Hossain is serving as an Editor for the IEEE TRANSACTIONS ON WIRELESS COMMUNICATIONS, and IEEE/KICS *Journal of Communications and Networks*. He is also serving as one of the Guest Editors for the Special Issue of the *Wiley Journal of Wireless Communications and Mobile Computing* on "Radio Link and Transport Protocol Engineering for Future-Generation Wireless Mobile Data Networks." He served as one of the Guest Editors for the Special Issue of the *Canadian Journal of Electrical and Computer Engineering* on "Advances in Wireless Communications and Networking." He was a recipient of the Lucent Technologies, Inc. research award for his contribution to the IEEE International Conference on Personal Wireless Communications (ICPWC), 1997.



Vijay K. Bhargava (S'70–M'74–SM'82–F'92) received the B.Sc., M.Sc., and Ph.D. degrees from Queen's University, Kingston, ON, Canada, in 1970, 1972, and 1974, respectively.

Currently, he is a Professor and Chair of electrical and computer engineering at the University of British Columbia, Vancouver, BC, Canada. He was also awarded a Tier I Canada Research Chair in Wireless Communications in 2001 which he held until 2003. He is a coauthor of the book *Digital Communications by Satellite* (New York: Wiley, 1981) and coeditor of

Reed-Solomon Codes and Their Applications (New York: IEEE Press, 1999) and *Communications, Information and Networking Security* (Boston, MA: Kluwer, 2002). His research interests are in multimedia wireless communications.

Dr. Bhargava is a recipient of the IEEE Centennial Medal (1984), IEEE Canada's McNaughton Gold Medal (1995), the IEEE Haraden Pratt Award (1999), the IEEE Third Millennium Medal (2000), and the IEEE Graduate Teaching Award (2002). He is very active in the IEEE and was nominated by the IEEE Board of Directors for the office of IEEE President-Elect in the year 2002 election. Currently, he serves on the Board of the IEEE Information Theory and Communications Societies. He is an Editor for the IEEE TRANSACTIONS ON COMMUNICATIONS and the IEEE TRANSACTIONS ON WIRELESS COMMUNICATIONS. He is a Past President of the IEEE Information Theory Society. He is a Fellow of the B.C. Advanced Systems Institute, Engineering Institute of Canada (EIC), the Canadian Academy of Engineering, and the Royal Society of Canada.